Potential involvement of 4-hydroxynonenal in the response of human lung cells to ozone

RAYMOND F. HAMILTON, JR.,[1] LI LI,[1] WILLIAM L. ESCHENBACHER,[2] LUKE SZWEDA,[3] AND ANDRIJ HOLIAN[1]

[1]*Division of Pulmonary and Critical Care Medicine, Department of Internal Medicine and Pharmacology Toxicology Program, University of Texas Medical School, and* [2]*Section of Pulmonary and Critical Care Medicine, Baylor College of Medicine, Houston, Texas 77030; and* [3]*Department of Physiology and Biophysics, Case Western Reserve University, Cleveland, Ohio 44106-4970*

Hamilton, Raymond F., Jr., Li Li, William L. Eschenbacher, Luke Szweda, and Andrij Holian. Potential involvement of 4-hydroxynonenal in the response of human lung cells to ozone. *Am. J. Physiol.* 274 (*Lung Cell. Mol. Physiol.* 18): L8–L16, 1998.—Ozone is a photochemically generated pollutant that can cause acute pulmonary inflammation and induce cellular injury and may contribute to the development or exacerbation of chronic lung diseases. Despite much research, the mechanisms of ozone- and oxidant-induced cellular injury are still uncertain. Ozone and secondary free radicals have been reported to cause the formation of aldehydes in biological fluids. One of the most toxic aldehydes formed during oxidant-induced lipid peroxidation is 4-hydroxynonenal (HNE). HNE reacts primarily with Cys, Lys, and His amino acids, altering protein function and forming protein adducts. The purpose of this study was to determine whether HNE could account for the acute effects of ozone on lung cells. Human subjects were exposed to 0.4 parts/million ozone or air for 1 h with exercise (each subject served as his/her own control). Six hours after ozone exposure, cells obtained by airway lavage were examined for apoptotic cell injury, and cells from bronchoalveolar lavage were examined for apoptosis, presence of HNE adducts, and expression of stress proteins. Significant apoptosis was evident in airway lung cells after ozone exposure. Western analysis demonstrated an increase in a 32-kDa HNE protein adduct and a number of stress proteins, viz., 72-kDa heat shock protein and ferritin, in alveolar macrophages (AM) after ozone exposure. All of these effects could be replicated by in vitro exposure of AM to HNE. Consequently, the in vitro results and demonstration of HNE protein adducts after ozone exposure are consistent with a potential role for HNE in the cellular toxic effects of ozone.

aldehydes; apoptosis; protein adducts; stress proteins; alveolar macrophages

OZONE is a photochemically generated pollutant that has been demonstrated to produce acute pulmonary inflammation and cellular injury. It has been proposed to contribute to the development or exacerbation of chronic lung diseases (20, 32). However, despite extensive investigation, the mechanism(s) of ozone-induced lung injury is not totally understood. Furthermore, not all of the effects of ozone on the lung cells have been clearly defined.

Aldehyde production as a result of ozone inhalation could be an important mediator of ozone toxicity (23). Furthermore, secondary radicals formed after ozone exposure could react with polyunsaturated fatty acids present in the lung lining fluid and cell membrane lipids to form hydrogen peroxide and aldehydes, of which the latter is considered to be more toxic (23). Although a large number of aldehydes can be formed during polyunsaturated fatty acid peroxidation, three aldehydes have been extensively studied as physiologically relevant lipid peroxidation products [4-hydroxynonenal (HNE), 4-hydroxyhexenal, and malonaldehyde]. Among the three, HNE is considered to be the most toxic aldehyde at the cellular level (7).

HNE has been shown to be formed in various models of inflammation and oxidative stress (24). In addition, we have recently shown that HNE is formed after ozone exposure, using murine and human models (10, 17). In human studies, ozone was shown to decrease alveolar macrophage (AM) function and to increase expression of 72-kDa heat shock protein (HSP72) in AM (10). Results from ozone exposure in murine models also demonstrated that ozone could induce apoptosis of lung cells (17). These results were consistent with studies indicating that HNE could induce HSP72 expression (3). Stress proteins, highly conserved between species, are a family of proteins synthesized when the cell is subjected to a variety of environmental assaults (e.g., heat, chemical, etc.), and they perform various functions to protect and adapt the cell to the stress condition (26). Stress protein induction could explain or contribute to the mechanism of adaptation that has been observed after repeated ozone exposures (9). Furthermore, in vitro studies with HNE using murine AM demonstrated that the effects of HNE could mimic those of ozone exposure and were dose dependent (17, 19). Low concentrations (5–25 μM) of HNE induced the stress protein heme oxygenase-1 (HO-1), 50–100 μM HNE induced apoptosis of AM, and higher concentrations of HNE caused cellular necrosis.

The purpose of the present study was to further test the hypothesis that HNE contributes to the effects of ozone injury. Human subjects were exposed to 0.4 parts/million (ppm) ozone or air for 1 h with exercise and then underwent both airway lavage (AL) and bronchoalveolar lavage (BAL) 6 h later. BAL cells were examined for evidence of stress protein expression, apoptosis, and formation of HNE-protein adducts. Due to limited cell yields, AL cells were examined for apoptosis only. In vitro studies were also conducted with human AM to determine whether HNE could mimic the effects of ozone.

METHODS

Study design. Detailed subject and ozone-exposure method descriptions are available elsewhere (12). All subjects were

1040-0605/98 $5.00 Copyright © 1998 the American Physiological Society

PM3006739413

Source: https://www.industrydocuments.ucsf.edu/docs/hsnx0001

healthy, nonsmoking volunteers who participated in this approved study after giving informed consent that was approved by the Institutional Review Boards of The Methodist Hospital, Baylor College of Medicine, and The University of Texas Houston Health Science Center. Each individual was evaluated with a complete history and physical examination and was screened for coagulation abnormalities. No subject had an upper respiratory tract infection within 6 wk before either exposure. Briefly, four human subjects received identical 1-h sham (air exposure) and 0.4 ppm ozone exposures with exercise 14 to 44 days apart. Subjects wore a noseclip and exercised continuously for 1 h on a cycle ergometer (type KEM-3; Mijnhardt, Odijk, The Netherlands) at a workload sufficient to achieve a minute ventilation of 30 $l \cdot min^{-1} \cdot m^2$ body surface area^{-1}. The order of exposure was randomized. Bronchoscopies, including BAL of the right middle lobe segment, were performed on all subjects after both air and ozone exposure 6 h after the termination of exposure. Concomitant with bronchoscopies, ALs were also performed on all subjects.

BAL and segmental AL. Six hours after exposure, subjects underwent bronchoscopy in a room adjacent to the exposure chamber in which O_2 and suction were available. No oral or parenteral premedication was used. The subjects were continuously monitored by pulse oximetry (OxyShuttle; Sensormedics, Anaheim, CA). Both nares were anesthetized with 2% Xylocaine jelly. Bronchoscopy was performed in the usual fashion without complications. Vocal cords were anesthetized using topical 1% Xylocaine in small boluses, with no more than 15 ml being used during the procedure. The bronchoscope was wedged in a right middle lobe segment, and lavage was performed with 35-ml aliquots of normal saline to a maximum of 140 ml. Subsequently, we performed the segmental AL with a custom-designed balloon catheter (no. 782015; Baxter, Santa Ana, CA) with two proximal infusion and withdrawal ports. The catheter was introduced through the nares not occupied by the bronchoscope and, under bronchoscopic visualization, was advanced to the left main stem bronchus. At this location, the balloon was inflated with adequate seal with no more than 2 ml of air. The bronchus was lavaged with 5-ml aliquots of normal saline until 5 ml of fluid were retrieved. The samples were immediately placed on ice and were transferred to the laboratory for analysis.

Cells were isolated from both AL and BAL and were examined for apoptosis, stress proteins, and HNE-protein adducts as described below. Cell counts were determined using a ZBI Coulter Counter (Coulter Electronics, Hialeah, FL). BALs from the study groups yielded an average of 6×10^6 cells that were >90% viable by trypan blue exclusion. ALs yielded between 0.1×10^6 and 1.0×10^6 cells.

Lung lavage and cell isolation. Lavage fluid was kept at 4°C until cells were isolated from the lavage fluid by a 4°C centrifugation at 1,500 revolutions/min (rpm; IEC centrifuge; Needham Heights, MA). The saline supernatant was aspirated, and the cell pellet was resuspended in a small volume (1–5 ml) of *N*-2-hydroxyethylpiperazine-*N*′-2-ethanesulfonic acid-buffered medium 199 (GIBCO BRL, Gaithersburg, MD) with 10% heat-inactivated fetal bovine serum (Sigma Chemical, St. Louis, MO) and added antibiotics (50 U/ml penicillin, 50 μg/ml gentamicin, and 50 μg/ml streptomycin). All culture media were pretreated with polymyxin B beads, removed before use, to ensure an endotoxin-free media. For in vitro cultures with HNE, 1×10^6 cells/ml were cultured at 37°C in the media described above for 4, 6, or 24 h in the presence and absence of variable concentrations of HNE. The HNE was pipetted directly into the cell culture from a 50 mM stock solution in absolute ethanol stored at −80°C. Cell cultures were maintained in suspension by slow end-over-end tumbling (Labquake Shakers; Labindustries, Berkeley, CA) in sterile polypropylene tubes (PGC Scientific, Gaithersburg, MD) at 37°C in a water-jacketed CO_2 incubator (Queue, Parkersburg, WV; see Ref. 25). Suspension cultures were selected for use in these studies rather than adherent cultures for the following reasons: *1*) they better model freshly isolated human AMs that were obtained by lung lavage because they were not adherent; *2*) adherence downregulates macrophage function (A. Helian, unpublished results) and may alter the response in these studies; and *3*) suspension cultures allow for a more uniform response and reliability with the assays in this study.

Cell viability assays (trypan blue exclusion). Cells in culture suspension were exposed to trypan blue dye [0.04% in phosphate-buffered saline (PBS)], placed on a hemocytometer, and examined under light microscopy. Two hundred random cells were counted after each treatment, and the percentage of blue cells was expressed as the percentage of nonviable cells for any given condition.

Morphological differentials. Immediately after cell isolation, 30×10^3 cells were placed in sterile disposable cytofunnels (Shandon, Cheshire, UK) and then were centrifuged at 1,500 rpm for 5 min onto positively charged glass slides (Probe On Plus; Fisher Scientific, Pittsburgh, PA) using a Shandon Cytospin 2 centrifuge. The cells were stained with Leukostat staining protocol as described below (Fisher Scientific). Differentials were performed at ×630 (dry objective) using a Zeiss microscope (Zeiss). Two hundred random cells were counted and were characterized as either macrophages, lymphocytes, neutrophils, eosinophils, or other. Cells obtained from all air-exposed and ozone-exposed subjects were >90% macrophages.

Apoptosis assays. Macrophage apoptosis was examined by a combination of Leukostat staining and detection of DNA fragmentation [Cell Death enzyme-linked immunosorbent assay (ELISA) and DNA ladder] in the cells. For Leukostat staining, cells were suspended in PBS (pH 7.2) at room temperature, cytocentrifuged onto positively charged microscope slides (Fisher Scientific) at 1,500 rpm for 5 min, fixed in cold methyl alcohol for 5 min, stained in Leukostat eosin stain for 2 min, and then stained in Leukostat methylene blue stain for 4 s. The slides were air-dried and were examined by light microscopy at ×630. For the detection of oligonucleosomes in cytoplasmic fractions (present during apoptosis) of the cells, the samples were processed and analyzed using the Cell Death Detection ELISA kit (Boehringer Mannheim, Indianapolis, IN) according to the manufacturer's protocol. The assay is based on the quantitative sandwich-enzyme-immunoassay principle using monoclonal antibodies directed against DNA and histone. Cells (1×10^5) from each sample were processed, 5,000 cells were used for each reaction, and triplicate reactions were performed for each sample.

To obtain DNA ladders, human AM were cultured with and without 50 μM HNE for 6 and 24 h as described above and were washed one time with PBS before DNA isolation. Genomic DNA was isolated by using the DNA ISOLATOR (Genosys, Woodlands, TX) according to the manufacturer's protocol. The isolated genomic DNA was dissolved in 10 mM tris(hydroxymethyl)aminomethane (Tris)-1 mM EDTA buffer (pH 8.0) and was 3′-end labeled with [α-^{32}P]dCTP (ICN Pharmaceuticals, Costa Mesa, CA) by incubation of 1 μg of DNA in 50 μl of reaction buffer (50 mM Tris·HCl, pH 7.6, 10 mM $MgCl_2$, 200 μM dATP, 200 μM dGTP, 200 μM dTTP, 2 μl of [α-^{32}P]dCTP, and 2 U Klenow) at 37°C for 30 min. The [α-^{32}P]dCTP-labeled DNA was mixed with 10 μl of loading buffer (0.25% bromphenol blue, 100 mM EDTA, and 30%

PM3006739414

Source: https://www.industrydocuments.ucsf.edu/docs/hsnx0001

glycerol). The same amount of [α-^{32}P]dCTP-labeled DNA (50 ng) was loaded onto a 2% agarose gel and was run at 5 V/cm for 5 h in 40 mM Tris-acetate buffer (pH 8.0) with 1 mM EDTA. The gel was dried at 60°C under vacuum conditions in a gel dryer and was exposed to X-ray film for detection of resolved labeled DNA fragments.

Sodium dodecyl sulfate-polyacrylamide gel electrophoresis and Western blotting for stress proteins and HNE-protein adducts. Immediately after cell isolation, 5 × 10^5 cells were collected in a microcentrifuge tube (Eppendorf, Westbury, NY), and the pellet was treated with sodium dodecyl sulfate-polyacrylamide gel electrophoresis denaturing buffer (10 μl/1 × 10^5 cells) and placed in a boiling water bath for 5 min. The denatured sample was then vortexed, sonicated, and stored at −20°C until use. After being thawed, denatured cellular protein samples equivalent to 1 × 10^5 cells/lane were separated on 12% Ready Gels (Bio-Rad, Hercules, CA) using a minigel apparatus (Bio-Rad). Resolved proteins were transferred to a nitrocellulose membrane (Amersham, Arlington Heights, IL) using a wet mini-transfer unit (Bio-Rad). The transferred blots were stained with 0.1% Ponceau S to determine uniform transfer and equal loading of the gels. The transferred blots were then incubated 16 h at 4°C in blocking buffer (5% Blotto in 10 mM Tris and 150 mM NaCl, pH 7.2). Membranes were then incubated with stress protein antibodies [HSP72, 65-kDa heat shock protein (HSP65), and HO-1 from StressGen, Victoria, BC, Canada, and ferritin from ICN Flow, Costa Mesa, CA] at a 1:2,000 dilution in blocking buffer for 18 h at 4°C or incubated with HNE adduct antibody (provided by L. I. Szweda and shown to recognize HNE-Cys, HNE-Lys, and HNE-His adducts; see Ref. 24) at a 1:500 dilution (24, 30) in blocking buffer for 18 h at 4°C and were washed extensively with Tris-buffered saline with 0.05% Tween 20 (TBST; pH 8.0). The membranes were then incubated with peroxidase-linked anti-mouse immunoglobulin (Ig; Amersham) at a 1:20,000 dilution for HSP72 (or peroxidase-linked anti-rabbit Ig at a 1:10,000 dilution for HO-1, HSP65, ferritin, and HNE-protein adducts) in TBST for 1 h at room temperature followed by extensive washing with TBST. The membranes were incubated in enhanced chemiluminescence (ECL) reagents (Amersham) for 1 min and were exposed to ECL film (Amersham) for 2 min that was developed by an automated film processor (Kodak, Rochester, NY). For all Western blots, the resulting exposed areas on the film were quantified by a scanning densitometer (BioImage; Milli-Cen/Biosearch, Division of Millipore, Bedford, MA), and the relative amounts of protein are expressed as integrated optical density (IOD).

The polyclonal antibody raised to HNE-modified keyhole-limpet hemocyanin was tested for cross-reactivity toward malondialdehyde (MDA) and sodium acetylcysteine (NAC) derivatives of acrolein, *trans*-2-pentenal (*t*2P), and *trans*-2-nonenal (*t*2N), which are compounds structurally similar to HNE. Competitive Western blot experiments and ELISA with these potential competitors were performed. Our results indicate that the anti-HNE antibody is highly specific to HNE-derived modifications to protein, exhibiting no binding to the Michael adducts of NAC-acrolein, -*t*2P, and -*t*2N or to MDA. In addition, antibody binding requires the presence of the 4-hydroxyl group (29), is sensitive to the chain length of the modifying 4-hydroxy-2-alkenal (29), and, as judged by competitive ELISA experiments, recognizes Cys-, His-, and Lys-HNE adducts (30). The epitope recognized by the antibody appears to be the hemiacetal form of the HNE-derived portion of protein-HNE adducts.

Statistical analysis. Due to subject variability, stress protein Western blot analysis IOD values were normalized by dividing each subject's ozone-exposed value by his/her air-exposed value, and these values were averaged. A one-tailed Student's *t*-test was then applied for each stress protein using one-sample hypothesis testing, assuming the population mean equaled one. For HNE adduct Western blots, there was no need to normalize the IOD values, and these data were analyzed by a paired one-tailed Student's *t*-test (air vs. ozone). Because of high background optical density (OD) values, Cell Death ELISA OD values were normalized by subtracting each subject's ozone-exposed value from his/her air-exposed value, and these values were averaged. Again, a one-tailed Student's *t*-test was then applied using one-sample hypothesis testing, assuming the population mean equaled zero.

RESULTS

Evidence for HNE formation after ozone exposure. To determine whether HNE was formed during in vivo ozone exposure in humans, AM obtained by BAL were examined for HNE protein adducts by Western analysis as described in METHODS. Figure 1 shows the Western blot obtained for HNE-protein adducts. The appearance of various HNE-adducted proteins was common in controls and probably represents constitutive HNE adducts due to the normal oxidizing environment of the lung. Similar to earlier studies with human and murine ozone exposures, the dominant feature after ozone exposure was a consistent increase in a 32-kDa protein adduct in each subject. The results from densitometry scans for the 32-kDa protein adduct are presented in Fig. 2. Although the increase in HNE-protein adducts did not achieve statistical significance ($0.1 \leq P \leq 0.5$), this result in combination with previous findings in the human (10) and murine (17) systems provides strong evidence for ozone-induced formation of HNE and its reaction with cell proteins.

AM stress protein expression after ozone exposure. We have previously shown that ozone could induce HSP72 levels in human AM after ozone exposure (10). To determine whether ozone exposure induced a stress response characteristic of oxidative stress, HSP72, HSP65, HO-1, and ferritin levels in AM were quanti-

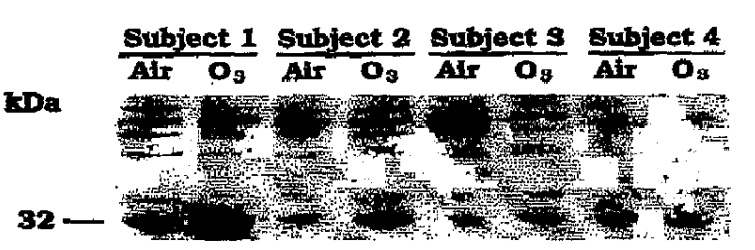

Fig. 1. 4 Hydroxynonenal (HNE)-protein adducts in alveolar macrophages (AMs) 6 h after exposure to 0.40 parts/million (ppm) ozone in 4 subjects. AMs were isolated from each of 4 subjects, and Western blot analysis for HNE-protein adducts in the cells was conducted as described in METHODS. Most clearly evident was an increase in an adducted protein at ~32 kDa. Conditions for each subject are labeled air and O_3 exposure.

PM3006739415

Source: https://www.industrydocuments.ucsf.edu/docs/hsnx0001

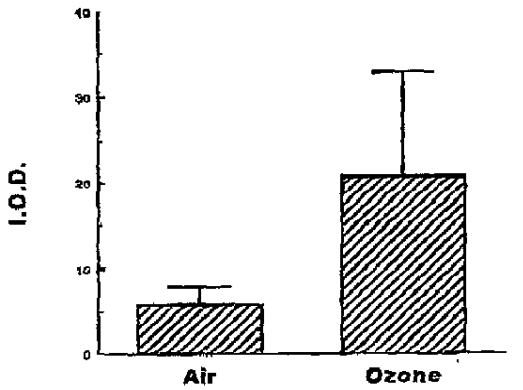

Fig. 2. Integrated optical density (IOD) values for the HNE-adducted 32-kDa protein shown in Fig. 1. Intensity of the 32-kDa protein was measured using a densitometer for each subject. Data are presented as means ± SE for 4 subjects.

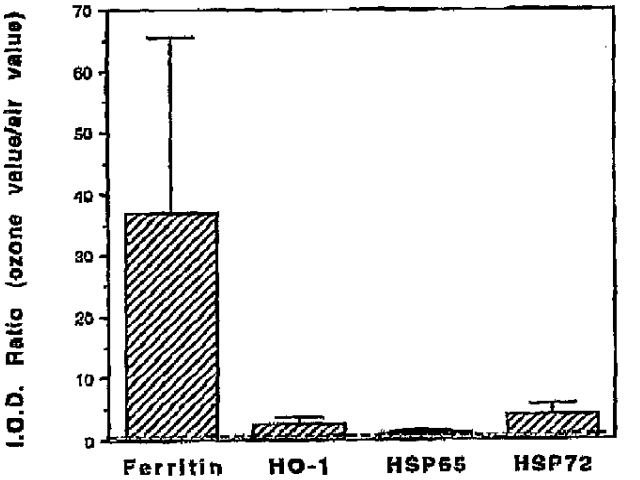

Fig. 4. Relative stress protein levels in bronchoalveolar lavage (BAL) cells from Fig. 3. Data are expressed as a ratio of IOD obtained from Western blot results. For each subject, ozone-exposed values were divided by the air-exposed values, and resulting ratios were averaged. Results are expressed as means ± SE for 4 subjects. HO-1, heme oxygenase-1.

tated after air and ozone exposures. The results of in vivo stress protein induction are illustrated in Fig. 3, and densitometry results for these Western blots are shown in Fig. 4. Consistent with previous studies, there was a variable fourfold increase in HSP72 after ozone exposure (10). Expression of HO-1 increased in two subjects and remained unchanged in two subjects after ozone exposure (Western blots not shown). In contrast, there was no apparent net change in HSP65 protein after ozone exposure. However, the stress protein most effected by ozone exposure was ferritin, which showed a variable but consistent increase for all subjects exposed to ozone. These results extend earlier studies by demonstrating that a stress protein traditionally associated with oxidative stress (i.e., ferritin) was also induced after ozone exposure.

AM stress protein expression after in vitro HNE exposure. HSP72, HSP65, HO-1, and ferritin levels in AM were quantitated to determine whether HNE exposure could induce a stress response in human AM in vitro in a similar manner to in vivo ozone exposure. Human AM were incubated with 0, 5, or 10 μM HNE for 4 h at 37°C. Representative results of in vitro stress protein induction by HNE from Western blot analysis are shown in Fig. 5. Results for HSP72 have been presented elsewhere (10). These results illustrate that a number of stress proteins can be induced by HNE in vitro. Furthermore, stress proteins could be induced at relatively low concentrations of HNE, i.e., ≤5 μM HNE. The response at low concentrations of HNE was maximal because higher concentrations (20–50 μM) did not further enhance stress protein expression (data not shown). Concentrations of HNE >50 μM produced no increase in stress proteins compared with control (data not shown).

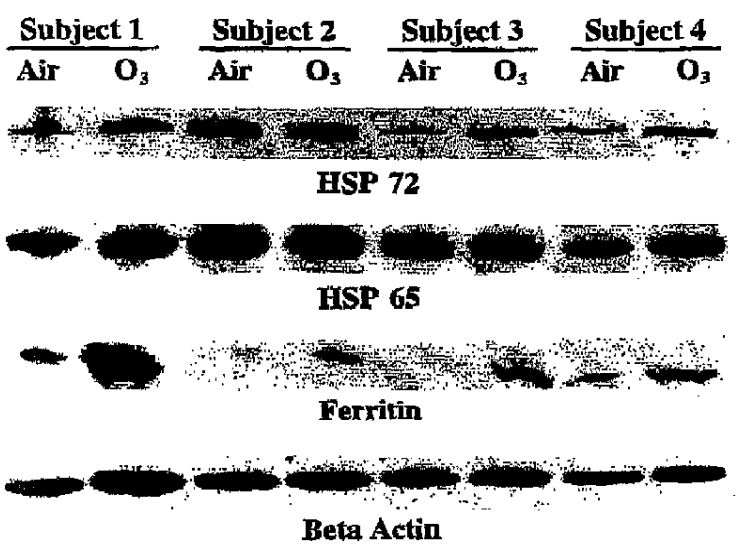

Fig. 3. Expression of 72-kDa heat shock protein (HSP72), 65-kDa heat shock protein (HSP65), and ferritin in AMs 6 h after 0.4 ppm ozone exposure compared with air exposure. Western blot analysis for each of the stress proteins and β-actin (representing protein loading in each lane) was conducted as described in METHODS. Each Western blot shows the results from the 4 subjects in the study. Although not statistically significant due to variance, ozone exposure induced the expression of HSP72 and ferritin in every subject.

PM3006739416

Source: https://www.industrydocuments.ucsf.edu/docs/hsnx0001

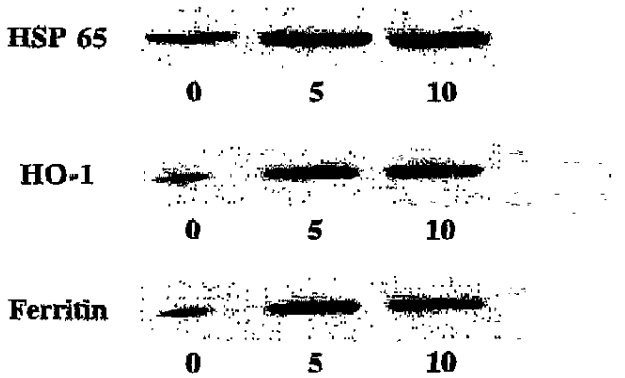

Fig. 5. Dose response for induction of stress proteins in bronchoalveolar cells in vitro. Results are representative Western blots illustrating HNE induction of HSP65, HO-1, and ferritin. Human AM cells were incubated 4 h at 37°C with different amounts (0, 5, 10 μM) of HNE, and then the cell samples were analyzed for stress protein expression in a similar manner as in Fig. 3. Results are representative of 2 experiments.

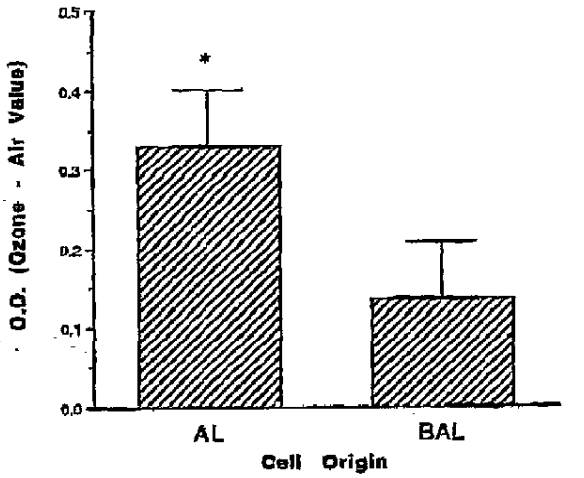

Fig. 7. Cell Death enzyme-linked immunosorbent assay (ELISA) results for airway lavage (AL) and BAL cells after 0.4 ppm ozone exposure. Both airway lung cells and AMs were assayed for apoptosis 6 h after air and ozone exposure by Cell Death ELISA as described in METHODS. Data are expressed [optical density (OD)] as means ± SE of 4 subjects' ozone minus air values. *$P < 0.05$ compared with a hypothetical mean of 0.

Lung cell apoptosis after ozone exposure. We have previously demonstrated that HNE could induce AM apoptosis in vitro in a murine model (19). Therefore, the effects of ozone exposure on human lung cell apoptosis were examined. Figure 6 is a representative morphological illustration of apoptosis in airway lung cells after ozone exposure. Figure 6*A* is a photomicrograph of cells obtained by AL after air (sham) exposure. Figure 6*B* is a photomicrograph of AL cells from the same subject after 0.4 ppm ozone exposure. In contrast to Fig. 6*A*, airway cells exposed to ozone showed a general shrinkage with a darkened, condensed nucleus, suggesting apoptotic cell injury. Some cells remained unaffected and have the appearance of control, air-exposed cells. In contrast, there was no significant morphological evidence of apoptosis in BAL cells after ozone exposure (data not shown).

To further examine whether airway lung cells were undergoing apoptosis after ozone exposure, the cells were assayed for apoptosis by Cell Death ELISA. Figure 7 shows the results of AL and BAL cells as quantified by Cell Death ELISA. Data are expressed as the average of ozone-exposed values with the air-exposed value subtracted. Consistent with the morphological evidence, there was a significant increase in cytosolic DNA fragments in AL cells after ozone. Simi-

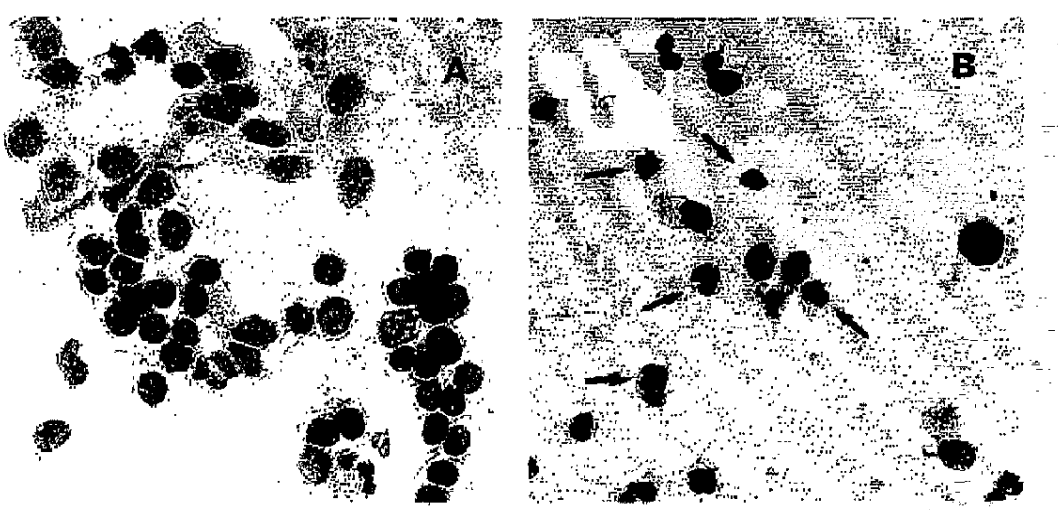

Fig. 6. Photomicrographs (×630) of airway lung cells isolated 6 h after air (sham) exposure (*A*) or 0.40 ppm ozone exposure (*B*). Airway cells were isolated and then were stained with Leukostat as described in METHODS. Results are representative of 4 subjects. Cells displaying nuclear condensation and cell shrinkage (consistent with morphological evidence of apoptosis) are indicated by arrows.

PM3006739417

Source: https://www.industrydocuments.ucsf.edu/docs/hsnx0001

lar to the results from morphology, BAL cells exhibited only a marginal but nonsignificant increase in DNA fragmentation.

AM apoptosis after in vitro HNE exposure. To test whether HNE could induce apoptosis, we exposed human AM to HNE in vitro and measured apoptosis by several methods. Cell Death ELISA is a very sensitive and early measure of apoptosis. Morphological changes can also appear relatively early, and these changes are the hallmark of apoptotic cells. DNA ladder formation is a late step in apoptosis and is an excellent confirmatory method when enough cells are available. Figure 8, *A* and *B*, is a photomicrograph of control and HNE-treated AM incubated for 24 h, respectively. AM shown in Fig. 8*A* have normal cell and nuclear appearance. HNE-exposed AM shown in Fig. 8*B* display nuclear condensation characteristic of apoptosis. Figure 9 shows the results from Cell Death ELISA from cells incubated for 6 h with HNE. The results clearly indicate that apoptosis in human AM is HNE dose dependent. Apoptosis was maximal at 50 μM HNE, whereas the highest concentration of HNE (100 μM) produced less DNA fragmentation. The results at 100 μM HNE suggested a necrotic process rather than an apoptotic process due to excessive HNE toxicity. The results shown in Fig. 10 further demonstrate that HNE induced apoptosis because characteristic DNA ladder formation was evident after a 24-h culture with 50 μM HNE.

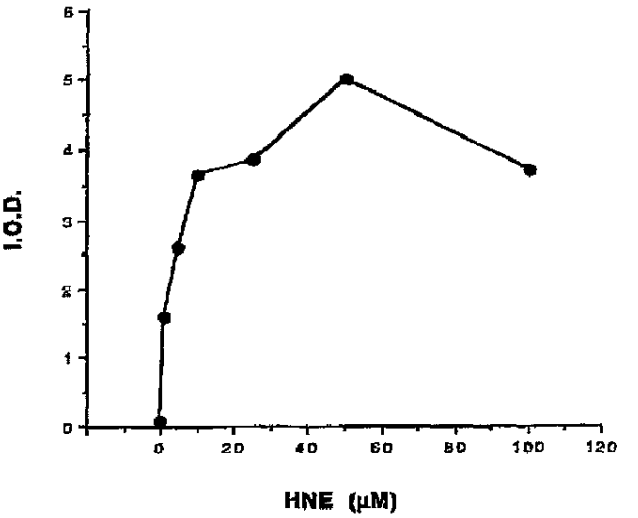

Fig. 9. Dose response of HNE-induced apoptosis of human AMs. Cell Death ELISA was used to quantitate apoptosis in a similar manner as in Fig. 7. AMs were incubated with increasing concentrations of HNE for 6 h at 37°C. Results indicate a dose-dependent increase in cytosolic DNA fragments in cultured AMs with increasing concentrations of HNE ($n = 1$).

DISCUSSION

This study examined two effects of acute ozone exposure (stress response and apoptosis) on human AM and apoptosis on airway lung cells to determine whether these effects could have been mediated by HNE. The results demonstrated that the effects of ozone on lung cells are consistent with the action of HNE. In addition, the results support the hypothesis that the cell injury and inflammation that occur after ozone exposure can be explained by initiation of lipid peroxidation and formation of toxic aldehydes such as HNE. The source of the oxidants that initiate HNE formation from polyunsaturated fatty acids such as arachidonic and linolenic acids cannot be distinguished at this time. It is possible that HNE formation may be secondary to the formation of free radicals by ozone in the lung lining layer. It is also possible that initiation of inflammation could trigger lipid peroxidation. We suspect that the latter suggestion is less likely because HNE was formed preceding recruitment of neutrophils in human exposures and in a murine model (17). Nevertheless, it is

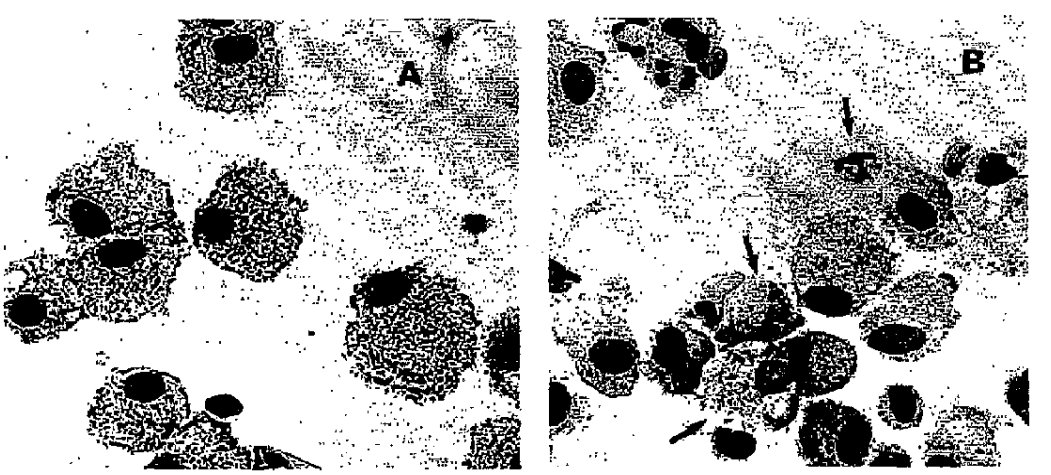

Fig. 8. Photomicrographs (×630) of AM cells after a 24-h control culture (A) or 50 μM HNE culture (B). Cells were stained in a similar manner as in Fig. 6. Apoptotic cells are indicated by arrows. Results are representative of 3 experiments.

PM3006739418

Source: https://www.industrydocuments.ucsf.edu/docs/hsnx0001

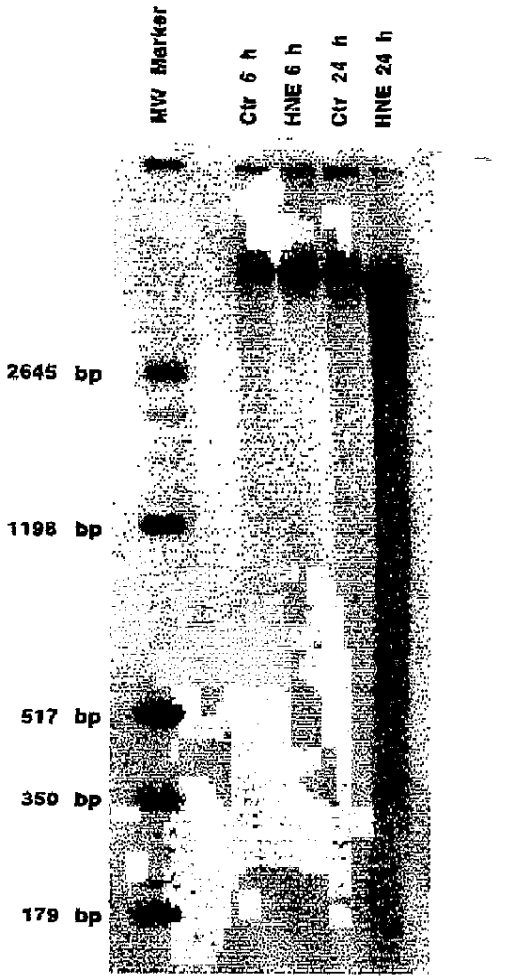

Fig. 10. Confirmation of HNE-induced apoptosis in human AMs. AMs were cultured for 6 and 24 h at 37°C with 50 μM HNE. Genomic DNA was isolated and analyzed as described in METHODS. Results are representative of 2 experiments. MW, molecular weight; Ctr, control.

evident that HNE is formed after ozone exposure and that HNE induces cellular effects very similar to those caused by ozone.

The cytotoxic effects of HNE most likely occur because of the high reactivity of HNE with certain amino acids (viz., Cys, Lys, and His), resulting in the formation of Michael's adducts (8). When these adducts occur in active sites or regulatory regions of proteins, then the function of those proteins can be altered (4–6, 13). If this occurs in one or more key cellular proteins, then alteration of cell function, induction of stress proteins, and/or cell injury could occur.

Evidence that HNE may be inhibiting specific and key proteins comes from recent studies of enzyme inhibition by HNE (21). In addition, we have recently demonstrated that HNE inhibits the cysteine protease interleukin (IL)-converting enzyme in an in vitro model (4). HNE inhibits the release of IL-1β from human monocytes (4) and macrophages (10). This specific effect of HNE could explain the inhibition of IL-1β release from AMs isolated from human subjects exposed to ozone (10). Consequently, in vitro and in vivo studies suggest that HNE is formed as a result of oxidant exposures and that key proteins can be targets for HNE.

In this study, we observed the consistent increase of a 32-kDa HNE protein adduct in AMs 6 h after ozone exposure. This finding extends preliminary results obtained in another study (10). In addition, the principal HNE-protein adduct detected after ozone exposure in a murine model was also a 32-kDa protein (17). The half-life of HNE-protein adducts can be estimated from the murine studies (17) to be on the order of 4–12 h. Therefore, the adducts could have been formed early during or after ozone exposure from secondary lipid peroxidation and could still be present at the 6-h time point in this study. The identity of this protein is unknown, and consequently it is not clear whether it is associated with the effects of HNE on AMs. However, it does appear to be a key target for HNE from in vivo ozone exposures and has the potential to serve as a biomarker for ozone exposure. However, because the formation of HNE is not specific to ozone, it is not certain how specific this 32-kDa HNE-protein adduct would be to ozone. A number of key enzymes have molecular masses of ~32 kDa, including HO-1. Identification of this protein may help explain the mechanism of oxidative stress on macrophages.

Oxidative stress can result in the induction of a number of proteins, collectively referred to as a stress response (3, 15, 16, 32). Induction of these proteins causes cells to become more resistant to subsequent environmental stressors (1, 18, 27, 28). We had previously reported that HSP72 was induced after ozone exposure (10). In this study, those findings were extended to include induction of ferritin, a protein known to be induced after oxidative stress (31). HO-1 and HSP65 were not consistently induced (Figs. 3 and 4). In vitro, HNE induced all four of these stress proteins (Fig. 5). There are a number of explanations for the difference between the in vitro HNE and in vivo ozone results. HO-1 is induced at low doses of HNE, whereas at higher doses of HNE, HO-1 is no longer induced (19). It appears that at higher concentrations of HNE, in which cytotoxic effects begin, HO-1 is no longer induced. Preliminary studies in C57BL/6 mice exposed to ozone demonstrated that HO-1 was induced at low ozone exposures (≤0.4 ppm for 3 h), but no HO-1 induction was observed at higher ozone exposures (data not shown). Therefore, HO-1 induction may be very susceptible to excess oxidative stress, and the dose of ozone in the present study may have been too high. Alternatively, other reactive aldehydes are also formed from lipid peroxidation and may have somewhat different effects on stress protein expression or may have acted in an additive manner, blocking HO-1 and HSP65 expression. Differences between the two models may also be due to the time course of exposure to HNE. In the in vivo model, HNE was probably formed over an

PM3006739419

Source: https://www.industrydocuments.ucsf.edu/docs/hsnx0001

extended time period (even after the cessation of ozone exposure), whereas in the in vitro model, HNE was added as a bolus. Consequently, the effects on specific stress protein expression may be altered. However, it is clear that both ozone and HNE induce the formation of multiple members of the stress protein family.

The implications of stress protein expression in human lung cells after ozone exposure are that they are a clear and quantifiable indicator of the presence of a significant environmental stress. In addition, the stress response is a protective mechanism against subsequent environmental stress. Although low levels of ozone exposure have distinct effects within cells, they may also protect the cells against subsequent ozone exposure. This protection may contribute to the adaptation observed after multiple ozone exposures (2, 9, 22).

A significant new finding from these studies is that modest ozone exposures can induce apoptosis in human lung cells. The apoptosis was evident from morphological appearance and from Cell Death ELISA results. Previous studies have demonstrated that the Cell Death ELISA assay is a sensitive and reliable indicator of apoptosis (11, 14, 19). Apoptosis was clearly evident in airway cells but not in peripheral lung cells obtained by BAL. It should be noted that although the increase in the Cell Death ELISA results was not significant in AMs, there was an increase, suggesting that even at this ozone exposure, minor cytotoxic events are beginning. In addition, in vitro studies confirmed that HNE could induce apoptosis of AMs. HNE induced morphological changes consistent with apoptosis, a dose-dependent increase in Cell Death ELISA results, and a DNA ladder typical of cells undergoing apoptosis. Therefore, both ozone in vivo and HNE in vitro can induce apoptosis of human lung cells, demonstrating the adverse health effects of ozone exposure.

The finding that only airway cells underwent significant apoptosis is consistent with the prediction that upper airway cells would be exposed to a higher concentration of ozone than the peripheral lung cells would receive. Furthermore, these results along with our previous in vitro and in vivo studies using human monocytes (4) and macrophages (10) can provide some estimates on the levels of HNE that would have been required to induce the biological effects of stress protein expression, inhibition of IL-1β and induction of apoptosis. The fact that stress proteins were induced and IL-1β release was inhibited in AMs but no significant apoptosis was observed suggests that levels of HNE of ~5 μM could have been formed and could have generated the observed effects. In contrast, ~10 times higher levels of HNE (50 μM) would have to have been formed in the airways to induce apoptosis. These upper values are based on the assumption that the primary active component causing the biological effects was HNE. To the extent that other agents formed as a result of ozone exposure contributed to the observed effects, then the amount of HNE formed and its relative overall contribution would correspondingly decrease.

In summary, we have established that acute ozone exposure in humans can induce a stress response and apoptosis in lung cells. Airway cells demonstrated evidence of undergoing apoptosis that may be due to the higher concentrations of ozone in the airways versus lower concentrations of ozone reaching the more distal alveolar spaces where ozone produced a stress response. HNE-protein adducts were detected after ozone exposure, primarily of a yet-to-be-identified 32-kDa protein, confirming that HNE was formed as a result of ozone exposure. Finally, all of the responses observed after ozone exposure were mimicked by HNE in vitro, providing additional evidence for the potential role reactive aldehydes may play in mediating the biological effects of ozone exposure.

This work was supported in part by a grant from the Methodist Foundation and National Center for Research Resources Grant M01-RR-02558.

Address for reprint requests: A. Hollan, Dept. of Internal Medicine, Univ. of Texas Medical School, 6431 Fannin, Rm. 1.276, Houston, TX 77030.

Received 8 October 1996; accepted in final form 12 September 1997.

REFERENCES

1. **Applegate, L. A., P. Luscher, and R. M. Tyrrell.** Induction of heme oxygenase: a general response to oxidant stress in cultured mammalian cells. *Cancer Res.* 51: 974–978, 1991.
2. **Bassett, D. J., E. Bwen-Kelly, C. L. Elbon, and S. S. Reichenbaugh.** Rat lung recovery from 3 days of continuous exposure to 0.75 ppm ozone. *J. Toxicol. Environ. Health* 25: 329–347, 1988.
3. **Cajone, F., and A. Bernelli-Zazzera.** Oxidative stress induces a subset of heat shock proteins in rat hepatocytes and MH1C1 cells. *Chem. Biol. Interact.* 65: 235–246, 1988.
4. **Davis, D. W., R. F. Hamilton, and A. Holian.** 4-Hydroxynonenal inhibits interleukin-1β converting enzyme. *J. Interferon Cytokine Res.* 17: 205–210, 1997.
5. **Esterbauer, H.** Kinetics of the reaction of sulfhydryl compounds with alpha-beta-unsaturated aldehydes. *Monatsh. Chem.* 101: 782–810, 1970.
6. **Esterbauer, H., A. Ertl, and N. Scholz.** The reaction of cysteine with alpha-beta-unsaturated aldehydes. *Tetrahedron* 32: 285–289, 1976.
7. **Esterbauer, H., R. J. Shaur, and H. Zollner.** Chemistry and biochemistry of 4-hydroxynonenal, malonaldehyde and related aldehydes. *Free Radic. Biol. Med.* 11: 81–128, 1991.
8. **Friguet, B., E. R. Stadtman, and L. I. Szweda.** Modification of glucose-6-phosphate dehydrogenase by 4-hydroxy-2-nonenal. Formation of cross-linked protein. *J. Biol. Chem.* 269: 21639–21643, 1994.
9. **Gilmour, M. I., R. R. Hmieleski, E. A. Stafford, and G. J. Jakab.** Suppression and recovery of the alveolar macrophage phagocytic system during continuous exposure to 0.5 ppm ozone. *Exp. Lung Res.* 17: 547–558, 1991.
10. **Hamilton, R. F., M. E. Hazbun, C. A. Jumper, W. L. Eschenbacher, and A. Holian.** 4-Hydroxynonenal mimics ozone-induced modulation of macrophage function ex vivo. *Am. J. Respir. Cell Mol. Biol.* 15: 275–282, 1996.
11. **Hamilton, R. F., L. Li, R. Iyer, and A. Holian.** Asbestos induces apoptosis in human alveolar macrophages. *Am. J. Physiol.* 271 (*Lung Cell. Mol. Physiol.* 15): L813–L819, 1996.
12. **Hazbun, M. E., R. Hamilton, A. Holian, and W. L. Eschenbacher.** Ozone-induced increases in substance P and 8-epi-prostaglandin $F_{2\alpha}$ in the airways of human subjects. *Am. J. Respir. Cell Mol. Biol.* 9: 568–572, 1993.
13. **Ishikawa, T., H. Esterbauer, and H. Sies.** Role of cardiac glutathione transferase and of the S-conjugate export system in biotransformation of 4-hydroxynonenal in the heart. *J. Biol. Chem.* 261: 1576–1586, 1986.
14. **Iyer, R., R. F. Hamilton, L. Li, and A. Holian.** Silica-induced apoptosis is mediated via scavenger receptor in human alveolar macrophages. *Toxicol. Appl. Pharmacol.* 141: 84–92, 1996.

PM3006739420

Source: https://www.industrydocuments.ucsf.edu/docs/hsnx0001

15. **Jornot, L., M. E. Mirault, and A. F. Junod.** Differential expression of hsp70 stress proteins in human endothelial cells exposed to heat shock and hydrogen peroxide. *Am. J. Respir. Cell Mol. Biol.* 5: 265–275, 1991.
16. **Keyse, S. M., and R. M. Tyrrell.** Both near ultraviolet radiation and the oxidizing agent hydrogen peroxide induce a 32-kDa stress protein in normal human skin fibroblasts. *J. Biol. Chem.* 262: 14821–14825, 1987.
17. **Kirichenko, A., L. Li, M. T. Morandi, and A. Holian.** 4-Hydroxy-2-nonenal protein adducts and apoptosis in murine lung cells after acute ozone exposure. *Toxicol. Appl. Pharmacol.* 141: 416–424, 1996.
18. **Kutty, R. K., R. F. Daniel, D. E. Ryan, W. Levin, and M. D. Maines.** Rat liver cytochrome P-450b, P-420b, and P-420c are degraded to biliverdin by heme oxygenase. *Arch. Biochem. Biophys.* 260: 638–644, 1988.
19. **Li, L., R. F. Hamilton, A. Kirichenko, and A. Holian.** 4-Hydroxynonenal-induced cell death in murine alveolar macrophages. *Toxicol. Appl. Pharmacol.* 139: 135–143, 1996.
20. **Mustafa, M.** Biochemical basis of ozone toxicity. *Free Radic. Biol. Med.* 9: 245–265, 1990.
21. **Parola, M., E. Albano, and R. Autelli.** Inhibition of the high affinity Ca^{2+}-ATPase activity in rat liver plasma membranes following carbon tetrachloride intoxication. *Chem. Biol. Interact.* 73: 103–119, 1990.
22. **Plopper, C. G., X. Duan, A. R. Buckpitt, and K. E. Pinkerton.** Dose-dependent tolerance to ozone. IV. Site specific elevation in antioxidant enzymes in the lungs of rats exposed for 90 days or 20 months. *Toxicol. Appl. Pharmacol.* 127: 124–131, 1994.
23. **Pryor, W. A., and D. F. Church.** Aldehydes, hydrogen peroxide, and organic radicals as mediators of ozone toxicity. *Free Radic. Biol. Med.* 11: 41–46, 1991.
24. **Quinn, M. T., J. C. Linner, D. Siemsen, E. A. Dratz, E. S. Buescher, and A. J. Jesaitis.** Immunocytochemical detection of lipid peroxidation in phagosomes of human neutrophils: correlation with expression of flavocytochrome b. *J. Leukoc. Biol.* 57: 415–421, 1995.
25. **Scheule, R. K., R. C. Perkins, R. F. Hamilton, and A. Holian.** Bleomycin stimulation of cytokine production by the human alveolar macrophage. *Am. J. Physiol.* 262 (*Lung Cell. Mol. Physiol.* 6): L386–L391, 1992.
26. **Schlesinger, M. J.** How the cell copes with stress and the function of heat shock proteins. *Pediatr. Res.* 36: 1–6, 1994.
27. **Stocker, R.** Induction of haem oxygenase as a defence against oxidative stress. *Free Radic. Res. Commun.* 9: 101–112, 1990.
28. **Stocker, R., Y. Yamamoto, A. F. McDonagh, A. N. Glazer, and B. N. Ames.** Bilirubin is an antioxidant of possible physiological importance. *Science* 235: 1043–1046, 1987.
29. **Uchida, K., K. Itakura, S. Kawakishi, H. Hiai, S. Toyokuni, and E. R. Stadtman.** Characterization of epitopes recognized by 4-hydroxy-2-nonenal specific antibodies. *Arch. Biochem. Biophys.* 324: 241–248, 1995.
30. **Uchida, K., L. I. Szweda, H. Chae, and E. R. Stadtman.** Immunochemical detection of 4-hydroxynonenal protein adducts in oxidized hepatocytes. *Proc. Natl. Acad. Sci. USA* 90: 8742–8746, 1993.
31. **Vile, G. F., S. Basu-Modak, C. Waltner, and R. M. Tyrrell.** Heme oxygenase 1 mediates an adaptive response to oxidative stress in human skin fibroblasts. *Proc. Natl. Acad. Sci. USA* 91: 2607–2610, 1994.
32. **Yamaguchi, M., H. Sato, and S. Bannai.** Induction of stress proteins in mouse peritoneal macrophages by oxidized low-density lipoprotein. *Biochem. Biophys. Res. Commun.* 193: 1198–1201, 1993.

Source: https://www.industrydocuments.ucsf.edu/docs/hsnx0001